European Journal of Medicinal Chemistry 75 (2014) 426–437

Contents lists available at ScienceDirect

European Journal of Medicinal Chemistry

journal homepage: http://www.elsevier.com/locate/ejmech

Original article

Development of GoSlo-SR-5-69, a potent activator of large conductance Ca^{2+}-activated K^+ (BK) channels

Subhrangsu Roy [b,1], Roddy J. Large [b,1], Adebola Morayo Akande [a], Aravind Kshatri [a], Tim I. Webb [b], Carmen Domene [c,d], Gerard P. Sergeant [a,b], Noel G. McHale [a,b], Keith D. Thornbury [a,b], Mark A. Hollywood [a,b,*]

[a] The Smooth Muscle Research Centre, Dundalk Institute of Technology, Dublin Road, Dundalk, County Louth, Ireland
[b] Ion Channel Biotechnology Centre, Dundalk Institute of Technology, Dublin Road, Dundalk, County Louth, Ireland
[c] Chemistry Research Laboratory, University of Oxford, Mansfield Road, Oxford OX1 3TA, UK
[d] Department of Chemistry, King's College London, Franklin-Wilkins Building, 150 Stamford Street, London SE1 9NH, UK

ARTICLE INFO

Article history:
Received 13 September 2013
Received in revised form
13 January 2014
Accepted 16 January 2014
Available online 3 February 2014

Keywords:
Ion channels
Anthraquinone derivatives
Ullmann coupling reaction
BK channel activator
Bladder

ABSTRACT

We have designed, synthesised and characterised the effects of a number of novel anthraquinone derivatives and assessed their effects on large conductance, Ca^{2+} activated K^+ (BK) channels recorded from rabbit bladder smooth muscle cells using the excised, inside/out configuration of the patch clamp technique. These compounds are members of the GoSlo-SR family of compounds, which potently open BK channels and shift the voltage required for half maximal activation ($V_{1/2}$) negatively. The efficacy of the anilinoanthraquinone derivatives was enhanced when the size of ring D was increased, since the cyclopentane and cyclohexane derivatives shifted the $V_{1/2}$, by -24 ± 6 mV and -54 ± 8 mV, respectively, whereas the cycloheptane and cyclooctane derivatives shifted the $V_{1/2}$ by -61 ± 6 mV and -106 ± 6 mV. To examine if a combination of hydrophobicity and steric bulking of this region further enhanced their ability to open BK channels, we synthesised a number of naphthalene and tetrahydro-naphthalene derivatives. The tetrahydro-2-naphthalene derivative GoSlo-SR-5-69 was the most potent and efficacious of the series since it was able to shift the activation $V_{1/2}$ by greater than -100 mV when applied at a concentration of 1 μM and had an EC_{50} of 251 nM, making it one of the most potent and efficacious BK channel openers synthesised to date.

1. Introduction

Large conductance Ca^{2+} activated (BK) channels are pore forming transmembrane proteins that play numerous roles in the excitability of neuronal [1–4] and muscle cells from mammals [5–7] through to nematodes [8–10]. In the lower urinary tract smooth muscles of mammals, BK channels contribute to the repolarisation phase of the action potential and thus modulate the influx of Ca^{2+} [5,11,12]. Since the mechanical activity of these smooth muscles is determined by the underlying electrical activity [13,14], the BK channels can contribute significantly to the resultant mechanical activity recorded in these tissues.

The role of these channels in the electrical and resultant mechanical activity of the urinary bladder has been extensively studied by a number of groups in experimental animals [7,11,13,14] and humans [15–17] and demonstrates that BK channels normally limit the influx of Ca^{2+} and thus reduces the contractile activity of the bladder. Interestingly, mice that have the pore forming BKα subunit genetically ablated [18], appear functionally incontinent, thus illustrating the important role these channels play in the control of bladder function. More recently, Hristov et al. [16], demonstrated that the expression of BK channels in human urinary bladder was significantly downregulated in patients suffering from neurogenic detrusor overactivity and suggested that the development of potent, efficacious BK channel openers may help offset the down-regulation of BK channels in these patients.

Over the past two decades, a number of novel BK channel openers have been developed [reviewed in Refs. [19–23]], but their efficacy in clinical trials appears limited [20], presumably due to their lack of effect at physiological membrane potentials (−80 mV to 0 mV). Consequently, we recently embarked on a study to

* Corresponding author. The Smooth Muscle Research Centre, Dundalk Institute of Technology, Dublin Road, Dundalk, County Louth, Ireland. Tel.: +353 429370475; fax: +353 429370509.
E-mail address: mark.hollywood@dkit.ie (M.A. Hollywood).
URL: http://www.smoothmusclegroup.org
[1] These authors contributed equally to this work and should be considered as joint first authors.

0223-5234/$ – see front matter © 2014 Elsevier Masson SAS. All rights reserved.
http://dx.doi.org/10.1016/j.ejmech.2014.01.035

develop a new family of BK channel openers (which we called the GoSlo-SR family [24],), in an attempt to produce more efficacious BK channel openers than those currently available. These anilinoanthraquinones were reasonably potent (EC_{50} ~2.5 μM) and shifted the voltage required for half maximal activation ($V_{1/2}$) of the BK channels by more than −100 mV, when applied (at a concentration of 10 μM) to excised patches of rabbit bladder smooth muscle plasma membranes. In contrast, the prototypical BK channel openers NS1619 [25] and NS11021 [26] only shifted the activation $V_{1/2}$ by approximately −25 mV and −50 mV respectively, when applied at the same concentration.

Our initial study of the structure activity relationship (SAR) of the GoSlo-SR molecules, suggested that the presence of an acidic group in 2-position of ring C was essential for BK channel agonist activity and that bulky and hydrophobic substituents on the phenyl ring D enhanced the efficacy significantly [24]. For example, the addition of a trifluoromethyl group in the *meta*-position of ring D (GoSlo-SR-5-6, Fig. 1) shifted $V_{1/2}$ by approximately −110 mV and the further addition of a methyl group in the *para*-position (GoSlo-SR-5-44, Fig. 1) increased this to approximately −140 mV, with little change in potency.

In the present study, we used the inside-out excised patch configuration of the patch clamp technique to examine the SAR of these compounds further in an attempt to (i) correlate how the size of ring D alters efficacy, (ii) ascertain if further alterations of the phenylamino ring at 4-position of C-ring enhance the efficacy and/or potency, and (iii) determine if the primary amine group at 1-position of ring C was essential for the BK channel opening activity. Our results suggest that the addition of tetrahydro-2-naphthylamine at the C-4 position of the basic anthraquinone core (to form GoSlo-SR-5-69) maintained efficacy but increased the potency by more than ten-fold, compared to the first generation GoSlo-SR series of molecules.

2. Chemistry

As shown in Scheme 1, the anilinoanthraquinone derivatives were prepared from commercially available bromaminic acid by Ullmann coupling reaction using two different methods [28,29]. The compounds **3**–**5** and **10**–**19** were obtained by a newly developed microwave assisted Ullmann coupling reaction in phosphate buffer using copper powder as a catalyst [28]. However, compounds **7** and **8** were synthesized by classical Ullmann coupling reaction in water in the presence of sodium carbonate and copper sulphate [29].

Scheme 2 demonstrates the synthesis of deaminated derivatives of 1-aminoanthraquinones **20**–**23** by using an efficient, one-pot, two-step reaction protocol recently reported in the literature [31]. The primary aromatic amine of 1-aminoanthraquinones was first diazotized by sodium nitrite and 1 M hydrochloric acid to obtain the stable, red coloured intermediate diazonium salt. The diazonium salt was further reduced by adding zinc powder in ethanol at

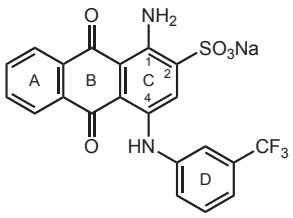

1 (GoSlo-SR-5-6)

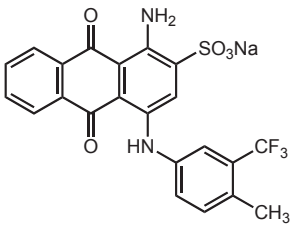

2 (GoSlo-SR-5-44)

Fig. 1. Structures of the first generation of GoSlo-SR compounds.

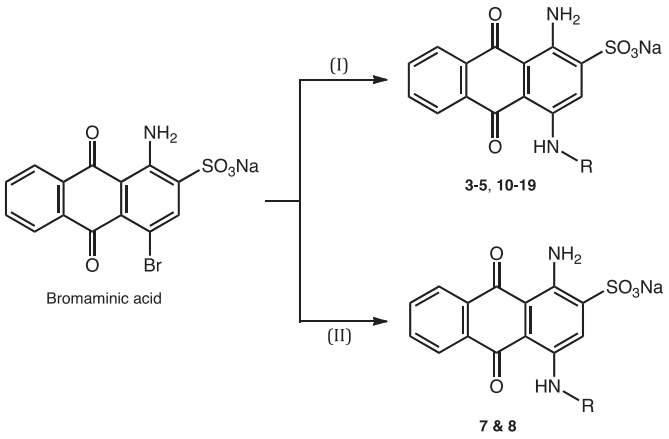

Scheme 1. Reagents and conditions: (i) R–NH_2, phosphate buffer, copper powder, microwave, 100–120 °C, 5–20 min; (ii) R–NH_2, Na_2CO_3, $CuSO_4$, water, 105 °C, 6–8 h.

room temperature. All the newly synthesized compounds (listed in Tables 1–3) were characterized by ^{1}H NMR, ^{13}C NMR and high-resolution mass spectral analysis. The purity of the compounds was determined by HPLC and their UV visible spectra and purity determinations are shown in the Supporting Information. With the exception of GoSlo-SR-5-90, which had a purity of 91.5%, all compounds had a purity of >95%.

3. Results and discussion

3.1. Single channel recording

In this study, we used the inside-out configuration of the patch clamp technique (see Experimental) with symmetrical 140 mM K^+ solutions, to evaluate the ability of a series of novel, GoSlo-SR family members (**3**–**23,** Tables 1–3) to open BK channels when applied to the cytosolic surface of membrane patches. As previously reported [24], the vast majority of current recorded under these conditions was due to activation of BK channels, since they (i) had a large conductance (~330 pS), (ii) shifted their voltage dependence of activation by approximately −100 mV, in response to a 10-fold increase in Ca^{2+} at the cytosolic face of the patch, (iii) reversed at the equilibrium potential for K^+ (0 mV), and (iv) were abolished in the presence of the selective BK channel inhibitors penitrem A [27] and iberiotoxin.

Membrane patches were held at −60 mV and voltage ramps (100 mV s^{-1}) were employed in these experiments to examine the effects of the novel BK channel openers on BK channels. The internal surface of the patch was continually bathed with 100 nM Ca^{2+} in the absence and presence of each test compound.

3.2. Effect of D ring size

We first assessed the effect of altering the cycloaliphatic D ring size on the efficacy of the molecules designed and synthesised

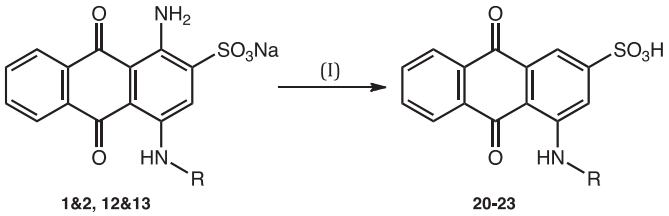

Scheme 2. Reagents and conditions: (i) (a) $NaNO_2$, HCl (1 M), 0 °C to rt, 1 h; (b) Zn, EtOH, rt, 5 min.

Table 1
Structure and effect of GoSlo-SR compounds on activation $\Delta V_{1/2}$. The substituents at each position are given in each column. All compounds were applied at 10 μM to the cytosolic surface of the patch in the presence of 100 nM Ca^{2+}. The change in voltage required for half maximal activation of the channels ($\Delta V_{1/2}$) is shown in the right hand column. Data are quoted as the mean ± standard error of the mean (SEM). Numbers in parentheses represent the number of replicates. Two of these molecules (**5** and **6**, denoted by [b]) have been previously reported to inhibit *ecto*-5′-nucleotidases [30] and the others are novel compounds.

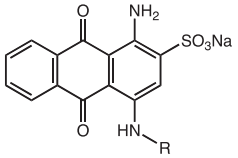

Compound	Name	R	$\Delta V_{1/2}$
3	GoSlo-SR-5-10		8 ± 6 (n = 5)
4	GoSlo-SR-5-20		−17 ± 6 (n = 5)
5[b]	GoSlo-SR-5-8		−24 ± 6 (n = 4)
6[b]	Acid Blue 62		−54 ± 8 (n = 4)
7	GoSlo-SR-5-32	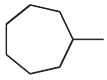	−61 ± 6 (n = 6)
8	GoSlo-SR-5-140	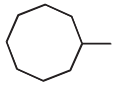	−106 ± 6 (n = 7)

following the Ullmann coupling reaction (Scheme 1) as reported in the literature [28,29]. We investigated if the cyclopropyl ring in the N^4-position activated the channels (**3**, GoSlo-SR-5-10, Table 1), but found that it had little effect, as illustrated by the typical record shown in Fig. 2A. In this and subsequent figures, the traces in grey and blue correspond to 100 nM Ca^{2+} in the absence and presence of the drug, respectively. The black trace represents the currents recorded in the presence of 1 μM Ca^{2+} and was used to estimate the number of BK channels in the patch. When a cyclobutyl ring was introduced to the N^4-position (**4**, GoSlo-SR-5-20) and added to the cytosolic face of the patch (Fig. 2B, blue trace) the activation $V_{1/2}$ was shifted negatively from 125 mV to 96 mV, whereas a 10-fold increase in Ca^{2+} shifted the $V_{1/2}$ to 8 mV. Introduction of a cycloheptane ring (**7**, GoSlo-SR-5-32, Fig. 2C) or a cyclooctane ring (**8**, GoSlo-SR-5-140, Fig. 2D) caused larger negative shifts in the activation $V_{1/2}$ from 133 mV to 53 mV and from 134 mV to 25 mV, respectively, suggesting that increasing the size of ring D enhanced the efficacy of the compounds on BK channels. Fig. 2E shows a summary of the shift in activation $V_{1/2}$ ($\Delta V_{1/2}$) plotted against the number of carbons in the D ring. Interestingly, the relationship was not linear, since increasing ring size from 4 to 5 carbons only shifted the mean $\Delta V_{1/2}$ by approximately −7 mV (from −17 ± 6 mV, n = 5 to −24 ± 6 mV, n = 4 respectively). Similarly when the effect of the cyclohexyl D ring was compared to that of the cycloheptyl ring, the $\Delta V_{1/2}$ also changed by only approximately −7 mV ($\Delta V_{1/2}$ with cyclohexyl was −54 ± 8 mV, n = 4 compared to −61 ± 6 mV, n = 6, with the cycloheptyl ring). In contrast, changing from a cyclopentyl to a cyclohexyl ring increased the $\Delta V_{1/2}$ from −24 ± 6 mV to −54 ± 8 mV and substitution of the cycloheptyl ring with the cyclooctyl ring changed the $\Delta V_{1/2}$ from −61 ± 6 mV (n = 6) to −106 ± 7 mV (n = 7). To examine if these effects could be correlated to the molecular size of each ring, we calculated the distance between C1′ of ring D and the most distal part of the D ring, as shown by the red arrow in Fig. 2D. As Fig. 2F suggests, when we plotted the size of the ring D against $\Delta V_{1/2}$ and fitted these data by linear regression, we obtained a reasonably good correlation (r^2 = 0.88) between D ring size and the $\Delta V_{1/2}$.

3.3. Effect of a ring fusion at different positions on the phenyl D ring

The above experiments suggested that the efficacy of the GoSlo-SR compounds could be enhanced by increasing the size of the ring D attached at the N^4-position. To examine if a combination of hydrophobicity and steric bulking of this region further enhanced the efficacy, we first assessed the effects of the tetrahydro-1-naphthalene (**10**, GoSlo-SR-5-65, Table 2) and 1-naphthalene (**11**, GoSlo-SR-5-103, Table 2) derivatives, where the cyclohexyl and phenyl ring was fused at the *ortho*- and *meta*-positions of the phenyl D ring respectively. These were then compared with the effects of the commercially available Acid Blue 25 (**9**, AB-25, Table 2). As Fig. 3B (blue trace) suggests, application of 10 μM AB-25 caused a negative shift in the activation $V_{1/2}$ of approximately −50 mV. When the data from five similar experiments were summarised (Fig. 3C), 10 μM AB-25 shifted the mean $V_{1/2}$ by −54 ± 4 mV (from 176 ± 13 mV to 122 ± 14 mV). However, compared to AB-25, compound **10** (GoSlo-SR-5-65, Fig. 3D–F) was twice as efficacious and the $V_{1/2}$ was shifted by −116 ± 9 mV (from −149 ± 10 mV to 33 ± 10 mV, n = 7) when applied at a concentration of 10 μM. Interestingly, as shown in Fig. 3H and I, compound **11** (GoSlo-SR-5-103, Table 2) was slightly less efficacious than AB-25, since it only shifted the $V_{1/2}$ by −44 ± 4 mV in eighteen experiments (from 142 ± 4 mV to 98 ± 5 mV) when applied at a concentration of 10 μM. These data suggest that the orientation and the conformation of the additional ring fused at the *ortho*- and *meta*-positions of the phenyl D ring play an important role in altering their efficacy on BK channels.

To examine if the position of the additional ring fused on phenyl D ring altered the effects of the compounds, we synthesised the tetrahydro-2-naphthalene (**12**, GoSlo-SR-5-69, Fig. 4D) and 2-naphthalene (**13**, GoSlo-SR-5-95, Fig. 4G) derivatives. Both of these compounds were found to be very potent and efficacious activators of BK channels as they negatively shifted the activation $V_{1/2}$ by more than −80 mV when applied at a concentration of 1 μM (Fig. 4E and H). In comparison, when 1 μM AB-25 (Fig. 4B, blue trace) was applied, the activation $V_{1/2}$ only shifted by −25 mV. In five similar experiments, summarised in Fig. 4C, 1 μM of AB-25 shifted the $V_{1/2}$ from 176 ± 13 mV (grey bar) to 150 ± 13 mV (blue bar), whereas compound **12** (GoSlo-SR-5-69) was approximately four times as efficacious and shifted the mean $V_{1/2}$ from 149 ± 7 mV (grey bar) to 46 ± 5 mV (blue bar, n = 10, Fig. 4F). Fig. 4H illustrates that compound **13** (GoSlo-SR-5-95) was moderately less efficacious than GoSlo-SR-5-69 and induced a negative shift in the activation $V_{1/2}$ of ∼ −80 mV. The lower efficacy was reflected in ten similar experiments summarised in Fig. 4I, where application of 1 μM of compound **13** shifted the activation $V_{1/2}$ from 151 ± 9 mV to 74 ± 10 mV. These data suggested that the fusion of either cyclohexyl or phenyl ring at *meta*- and *para*-positions of the phenyl D ring significantly enhanced the efficacy of the compounds.

To measure the potency of the compounds, we next performed a series of experiments in which increasing concentrations of each compound were applied to the cytosolic face of the BK channels in the continued presence of 100 nM Ca^{2+}. A typical experiment with GoSlo-SR-5-69 is shown in Fig. 5A. Under control conditions (100 nM Ca^{2+}, grey trace), the channels were half maximally activated at −130 mV. Increasing the concentration of GoSlo-SR-5-69 caused a concentration dependent, negative shift in the $V_{1/2}$. To summarise these data, we obtained the $\Delta V_{1/2}$ by subtracting the $V_{1/2}$ obtained in

Table 2
Structure, efficacy and potency of GoSlo-SR compounds on BK channels. The first column refers to the number of the compound and the second column refers to its family name. Each substituent at position N^4 is given in column 3. Compounds were applied at either 10 μM or 1 μM (as detailed in column 4) to the cytosolic surface of the patch in the presence of 100 nM Ca^{2+}. The change in voltage required for half maximal activation of the channels ($\Delta V_{1/2}$) and the concentration that produced half maximal effects (EC_{50}) is shown in the column 5. Data are quoted as the mean ± standard error of the mean (SEM) for $\Delta V_{1/2}$ or mean ± 95% confidence intervals for EC_{50} (column 5). '*n*' refers to the number of replicates. Three of these molecules (**9, 11** and **13**, denoted by [b]) have been previously demonstrated to inhibit P_2Y receptors or *ecto*-5′-nucleotidases [30] and the remainder are novel compounds.

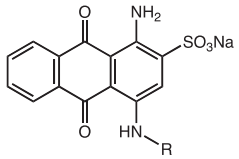

Compound	Name	R	$\Delta V_{1/2}$	EC_{50} (95% CI)
9[b]	Acid Blue 25	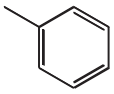	−54 ± 4 (n = 5)	5.9 μM (2.7–12.9 μM)
10	GoSlo-SR-5-65	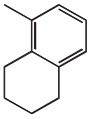	−116 ± 9 (n = 7)	366 nM (255–525 nM)
11[b]	GoSlo-SR-5-103	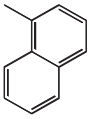	−44 ± 4 (n = 18)	841 nM (0.3–2.1 μM)
12	GoSlo-SR-5-69	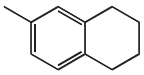	−104 ± 9, (n = 10) (1 μM)	251 nM (105–597 nM)
13[b]	GoSlo-SR-5-95	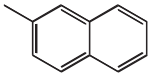	−85 ± 12 (n = 10) (1 μM)	392 nM (0.14–1.1 μM)
14	GoSlo-SR-5-64	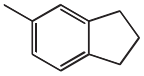	−88 ± 12 (n = 6)	2.9 μM (1.7–4.8 μM)
15	GoSlo-SR-5-124	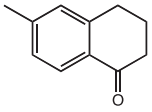	−66 ± 8 (n = 4)	N.D.
16	GoSlo-SR-5-7	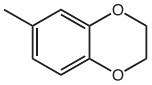	−14 ± 7 (n = 4)	N.D.
17	GoSlo-SR-5-90	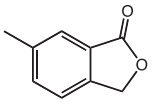	14 ± 8 (n = 5)	N.D.
18	GoSlo-SR-5-126	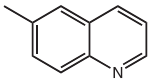	−26 ± 11 (n = 5)	N.D.
19	GoSlo-SR-5-127	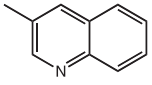	−38 ± 6 (n = 5)	N.D.

the absence of the drug (100 nM Ca^{2+}) from the $V_{1/2}$ measured in each concentration of the compound. Fig. 5B shows the summary of these data in which the $\Delta V_{1/2}$ was plotted against the concentration of GoSlo-SR-5-69 applied. When these data were fitted with the Langmuir equation, the concentration at which the compound had its half maximal effect (EC_{50}) was 251 nM (95% confidence intervals (CI) were 105–597 nM) and the Hill coefficient was 0.69 ± 0.16. In comparison, AB-25, shown in Fig. 5D, had an EC_{50} that was ~24-fold lower (5.9 μM, Hill coefficient was 0.7 ± 0.11, **9**, Table 2) than that of GoSlo-SR-5-69 (**12**, Table 2). As Fig. 5B–E suggest, the order of potency and efficacy was GoSlo-SR-5-69 > GoSlo-SR-5-65 > GoSlo-SR-5-95 >> AB-25, thus suggesting that the tetrahydro-2-naphthalene derivative **12** was the most potent and efficacious opener of this series. However, as shown in Fig. 5F, the 1-naphthalene derivative, **11**

Table 3
Structure, efficacy and potency of deaminated GoSlo-SR compounds on BK channels. The first column refers to the number of the compound and the second column refers to its family name. Each substituent at position N^4 is given in column 3. Compounds were applied at either 10 μM or 1 μM (as detailed in column 4) to the cytosolic surface of the patch in the presence of 100 nM Ca^{2+}. The change in voltage required for half maximal activation of the channels ($\Delta V_{1/2}$) and the concentration that produced half maximal effects (EC_{50}) is shown in the column 5. Data are quoted as the mean ± standard error of the mean (SEM) for $\Delta V_{1/2}$ or mean ± 95% confidence intervals for EC_{50} (column 5). *n* Refers to the number of replicates for the $\Delta V_{1/2}$ determination. For EC_{50} determinations, different concentrations were applied to between 5 and 30 patches for each compound, with the exception of 300 nM GoSlo-SR-5-103 and AB-25, which were applied to 4 and 2 patches, respectively. Compound **21** (GoSlo-SR-5-132) has been previously synthesised [31] but its biological activity has not been determined.

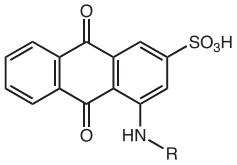

Compound	Name	R	$\Delta V_{1/2}$	EC_{50}
20	GoSlo-SR-5-134	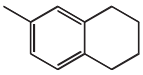	−79 ± 6 (*n* = 9) (1 μM)	640 nM (460–885 nM)
21[b]	GoSlo-SR-5-132	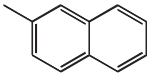	−41 ± 4 (*n* = 6) (1 μM)	984 nM (632–1.52 μM)
22	GoSlo-SR-5-130	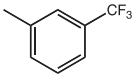	−97 ± 4 (*n* = 7)	1.8 μM (1.2–3.4 μM)
23	GoSlo-SR-5-138	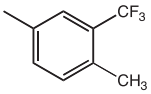	−115 ± 8 (*n* = 6)	964 nM (0.56–1.7 μM)

(GoSlo-SR-5-103, Table 2) had a reduced potency (EC_{50} = 841 nM) and efficacy compared to the 2-naphthalene derivative **13** (GoSlo-SR-5-95, EC_{50} = 392 nM, Table 2), suggesting that the position of the phenyl ring fused with phenyl D ring significantly altered the potency and efficacy of these molecules. Taken together, the data presented above suggest that both the orientation and the conformation of the additional ring fused with ring D markedly altered the efficacy and potency of these molecules.

Interestingly, when we reduced the size of the ring, fused with ring D, from cyclohexane to cyclopentane (**14**, GoSlo-SR-5-64, Table 2), the potency (assessed from the EC_{50}) was reduced by more than 10-fold to 2.9 μM and the efficacy was also modestly reduced compared to GoSlo-SR-5-69. Incorporation of either the polar functional group or polar atom(s) in the additional ring that attached with ring D, resulted in less efficacious compounds. Thus, the tetralone derivative **15** (GoSlo-SR-124, Table 2) significantly reduced the $\Delta V_{1/2}$ to −66 ± 8 mV ($n = 4$, $p < 0.05$) when applied at 10 μM. Similarly, the ability to open the BK channels with compounds **16**–**18** was dramatically reduced (see Table 2). Additionally, the incorporation of a nitrogen atom into the D ring (**19**, GoSlo-SR-5-127, Table 2) also reduced the efficacy to −38 ± 6 mV ($n = 5$, $p < 0.001$). These data clearly demonstrated that increasing the hydrophilicity, either of the D-ring or the ring fused with phenyl ring D reduced their ability to open BK channels significantly.

3.4. Effect of deaminated derivatives

We also examined the contribution of the primary amine present at 1-position of the C-ring to BK channel opening activity. However, compound **22** (GoSlo-SR-5-130, Table 3) shifted the activation $V_{1/2}$ by −97 ± 4 mV at a concentration of 10 μM and had an EC_{50} of 1.8 μM. Neither of these values was significantly different from the aminated form (**1**, GoSlo-SR-5-6) reported previously by us [24]. In contrast, the deaminated form of **2**, GoSlo-SR-5-44 [24], compound **23** (GoSlo-SR-5-138, Table 3) showed an increased potency (964 nM vs. 2.4 μM), but its efficacy was moderately reduced (−115 ± 8 mV, $p < 0.05$) compared to GoSlo-SR-5-44 [24]. When we examined the effects of the deaminated derivative of the most potent compound **12** (GoSlo-SR-5-69) of this series, compound **20** (GoSlo-SR-5-134, Table 3), we found the efficacy of GoSlo-SR-5-134 at 1 μM was significantly decreased (−79 ± 6 mV compared to −104 ± 8 mV, $p < 0.005$) and its potency was reduced more than two-fold compared to GoSlo-SR-5-69. The deaminated derivative of GoSlo-SR-5-95, compound **21** (GoSlo-SR-5-132, Table 3) was even less effective and shifted the activation $V_{1/2}$ by only −41 ± 4 mV ($n = 6$) at a concentration of 1 μM, with an EC_{50} of 984 nM. The data presented in Table 3 suggest that deaminated derivatives **20**–**23** had variable effects on the potency and the efficacy compared to their aminated forms. However, these data demonstrate that the primary aromatic amine group present at 1-position in the C-ring of the anilinoanthraquinone is not essential for opening BK channels.

It will now be of interest to examine the effects of these new BK channel modulators on mechanical activity in the bladder. However, before we do this, we will also need to carefully characterize the effects of these compounds on the other ion channels that are known to contribute to electrical activity in the bladder (ie Ca^{2+} channels, voltage-gated K^+ channels, K_{ATP} channels and calcium activated chloride channels). In addition, we will need to examine if the compounds have any effects on Ca^{2+} handling in smooth muscle cells, before we can reliably interpret the effects of the compounds on mechanical activity.

4. Summary

We have synthesised the second generation of GoSlo-SR molecules and examined their effects on BK channels in patches of membrane from rabbit bladder smooth muscle cells. The efficacy of these molecules was enhanced when the size of the ring D was increased. Furthermore, efficacy was maintained and potency enhanced by more

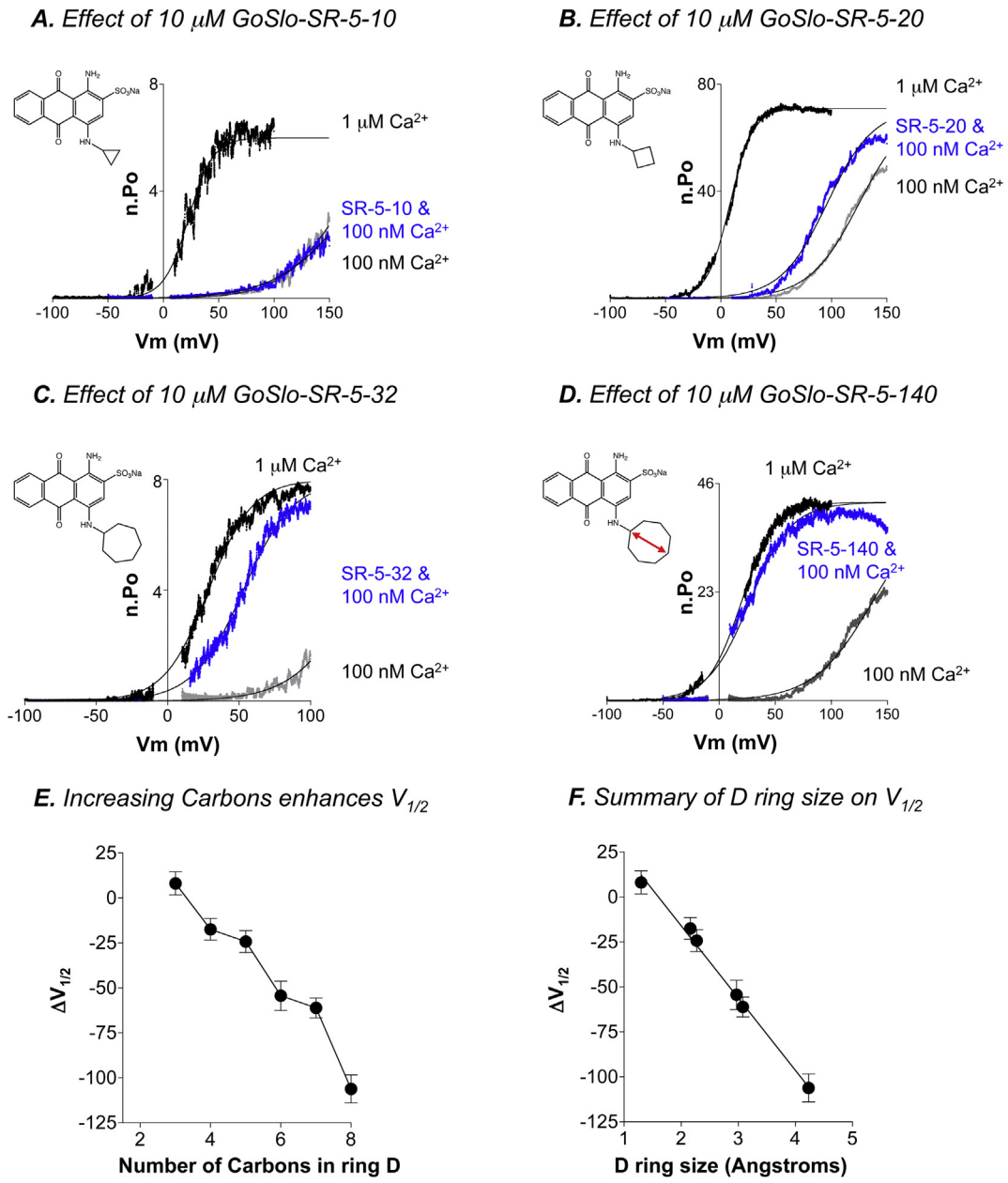

Fig. 2. Increasing D ring size enhances efficacy of the GoSlo-SR molecules as BK channel agonists. Fig. 2A–D shows BK currents evoked by voltage ramps in 100 nM Ca^{2+} before (grey traces) and during drug application (blue traces). The black traces show the effect of 1 μM Ca^{2+} on BK currents evoked by voltage ramps from −100 to +100 mV. Increasing Ca^{2+} at the cytosolic surface of the patch increased the number of channel openings and shifted the voltage at which they opened to more negative potentials. The structure of each molecule is shown in the inset in each panel. As (A)–(D) suggest, increasing the ring size enhanced the efficacy of each compound as evidenced by the negative shift in the current voltage relationships in the presence of each molecule. The filled lines represent the fit of the data with the Boltzmann equation. Panel E shows summary data in which the $\Delta V_{1/2}$ was plotted against ring size and illustrates that the relationship was not linear. Panel F shows summary data in which the size of the D ring (measured as shown by the red arrow in D) was plotted against $\Delta V_{1/2}$. The solid line in (F) shows the fit of the data obtained by linear regression. (For interpretation of the references to colour in this figure legend, the reader is referred to the web version of this article.)

than an order of magnitude when the D ring was substituted with tetrahydro-2-naphthalene. Deamination at 1-position on the C ring slightly reduced efficacy and potency suggesting that the primary amine group at this position is not obligatory for BK channel opening activity in rabbit bladder smooth muscle cells.

5. Experimental

5.1. Chemistry

All reagents and solvents were obtained from commercial sources and used without further purification. Proton nuclear magnetic resonance (^{1}H NMR) spectra and carbon nuclear magnetic resonance (^{13}C NMR) spectra were recorded on Bruker AMX 400 MHz and Bruker AMX 100 MHz NMR spectrometer, respectively, at 27 °C. All ^{1}H NMR chemical shifts are reported in δ units, parts per million (ppm) downfield of tetramethylsilane (TMS), and were measured relative to the signal for dimethylsulfoxide (2.50 ppm). Data for ^{1}H NMR are reported as follows: chemical shift (δ ppm), multiplicity (s = singlet, d = doublet, t = triplet, q = quartet, m = multiplet, br = broad), integration, and coupling constant (J Hz). Chemical shifts (δ) for carbon are reported in parts per million (ppm) downfield from tetramethylsilane (TMS) and are referenced to residual solvent peaks: carbon (DMSO-d_6 39.47 ppm).

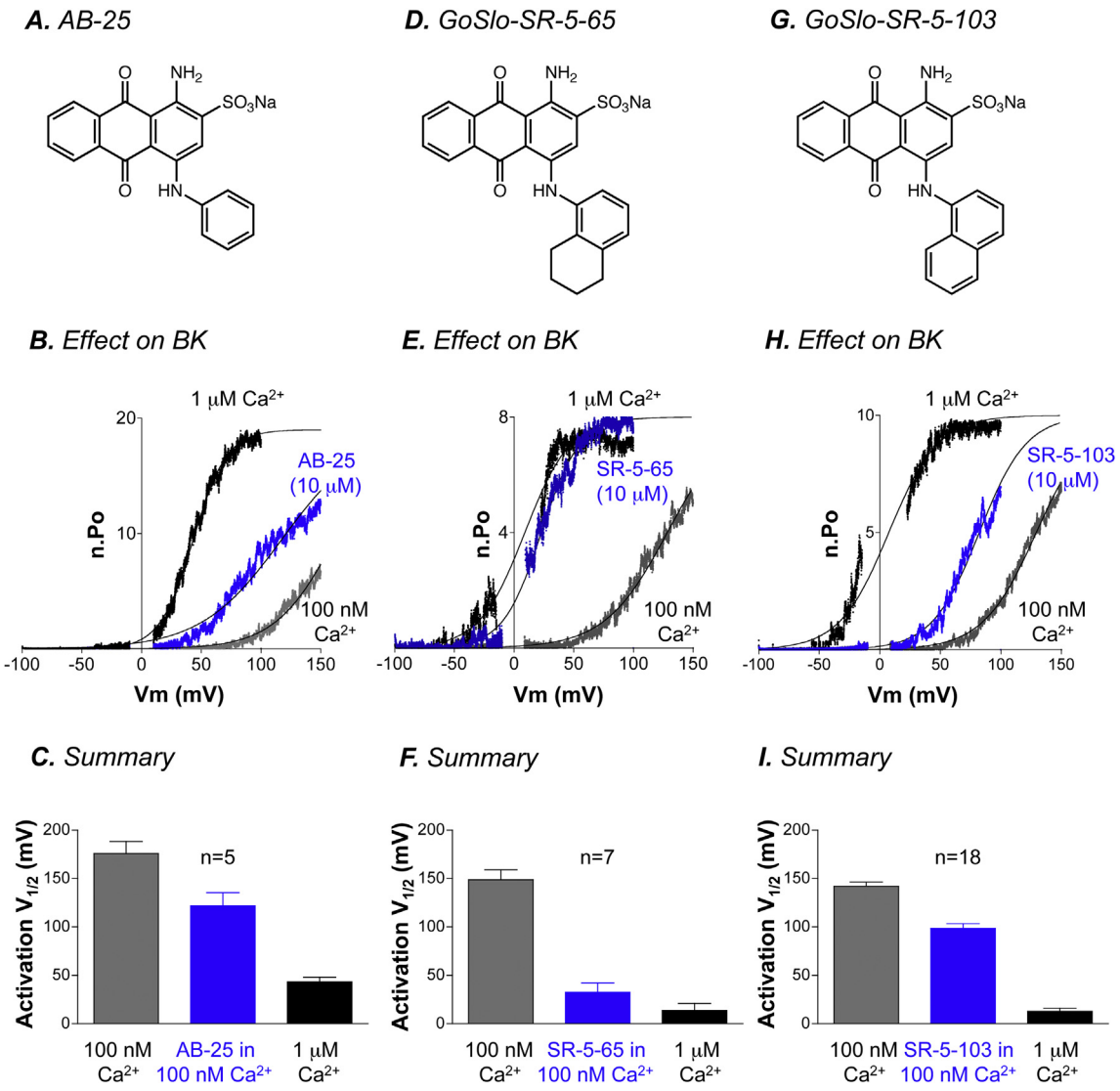

Fig. 3. Comparison of the effects of 10 μM AB-25, GoSlo-SR-5-65 and GoSlo-SR-5-103 on the activation of BK channels. Panels A, D and G show the structure of AB-25, GoSlo-SR-5-65 and GoSlo-SR-5-103, respectively. Panels B, E and H show the effect of 100 nM (grey traces) and 1 μM Ca^{2+} (black traces) on BK currents before application of 10 μM AB-25, GoSlo-SR-5-65 and GoSlo-SR-5-103, respectively, in the presence of 100 nM Ca^{2+} (blue traces). Solid lines show Boltzmann fits to the data. Panels C, F and I show summary bar-charts from separate experiments in which the mean $V_{1/2}$ in the presence of 100 nM Ca^{2+} (grey bars) and 1 μM Ca^{2+} (black bars) on patches before application of 10 μM AB-25 (blue bars, Panel C), 10 μM GoSlo-SR-5-65 (blue bars, Panel F) or 10 μM GoSlo-SR-5-103 (blue bars, Panel I). (For interpretation of the references to colour in this figure legend, the reader is referred to the web version of this article.)

The purities of isolated products were determined on Agilent 1200 series system (Agilent Technologies, Germany) using the following procedure: the compounds were dissolved at a concentration of 0.5 mg/mL in purified water:acetonitrile = 90:10 (% v/v), containing 0.1% trifluoroacetic acid (TFA). Sample (5 μL) was then injected into an Agilent Poroshell 120 EC-C18 column (100 × 3.0 mm I.D., 2.7 μm particle size). Elution was performed with a linear gradient of purified water:acetonitrile (containing for both mobile phases 0.1% TFA) from 90:10 (% v/v) to 20:80 (% v/v) during 17 min, then return to original conditions in 1 min, followed by keeping for re-equilibration at original conditions (90:10% v/v purified water:-acetonitrile containing 0.1% TFA) for 3 min, at a flow rate of 700 μL/min. UV absorption was detected from 200 to 750 nm using a diode array detector and the purity of the compounds was determined at 254 nm (see the Supporting Information). The School of Chemistry and Chemical Biology, University College Dublin recorded high Resolution Mass Spectra (HRMS) using a Micromass/Waters LCT instrument. Microwave reactions were carried out using a CEM focused™ Microwave Synthesis type Discover® apparatus. Reactions were monitored by analytical thin layer chromatography (TLC), which was performed on aluminium sheets pre-coated with silica gel 60 F_{254}, or aluminium sheets pre-coated with RP silica gel 18 F_{254} (Merck, Germany). Column flash chromatography was performed on Merck Kieselgel 60 (0.040–0.063 mm) or Silica gel $100C_{18}$-Reversed phase (Fluka, Switzerland). The columns, packed with Merck Kieselgel 60, were eluted with various combinations of ethyl acetate and methanol mixtures. The columns, packed with Silica gel $100C_{18}$-Reversed phase, were eluted with various combinations of water and methanol mixtures. A freeze-dryer (CHRIST ALPHA 1-4 LSC) was used for lyophilisation.

5.1.1. General procedure A: preparation of **3**–**5** and **10**–**19**

To a 30 mL microwave reaction vial, buffer solution of 0.2 M Na_2HPO_4 (3 mL) and 0.12 M NaH_2PO_4 (5 mL), bromaminic acid sodium salt (0.2 g, 0.495 mmol), a catalytic amount (~4 mg) of copper powder and the appropriate aniline or amine derivative

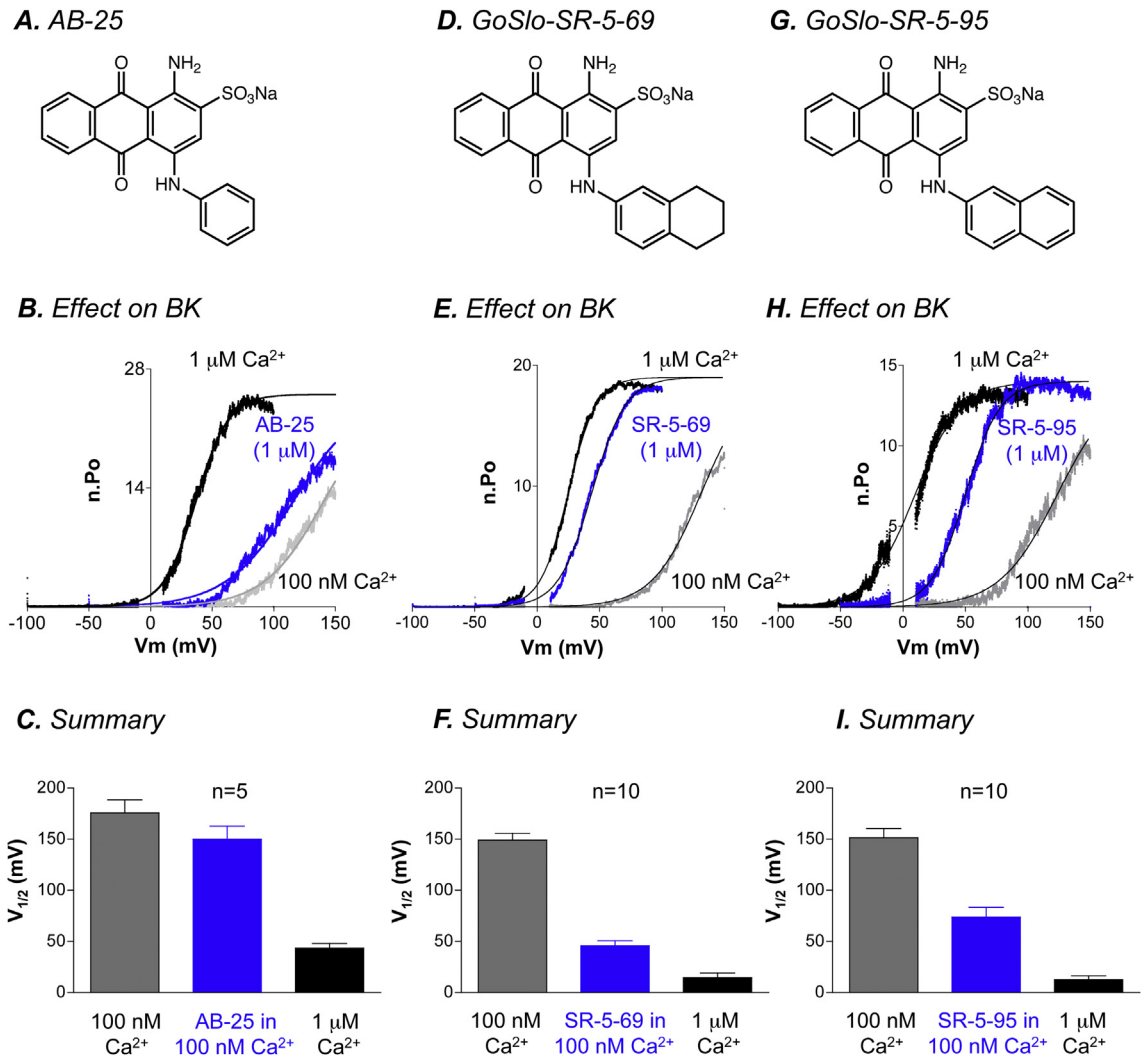

Fig. 4. Comparison of the effects of 1 μM AB-25, GoSlo-SR-5-69 and GoSlo-SR-5-95 on the activation of BK channels. Panels A, D and G show the structure of AB-25, GoSlo-SR-5-69 and GoSlo-SR-5-95, respectively. Panels B, E and H show the effect of 100 nM (grey traces) and 1 μM Ca^{2+} (black traces) on BK currents before application of 1 μM AB-25, GoSlo-SR-5-69 and GoSlo-SR-5-95, respectively, in the presence of 100 nM Ca^{2+} (blue traces). Solid lines show Boltzmann fits to the data. Panels C, F and I show summary bar-charts from separate experiments in which the mean $V_{1/2}$ in the presence of 100 nM Ca^{2+} (grey bars) and 1 μM Ca^{2+} (black bars) on patches before application of 1 μM AB-25 (blue bars, Panel C), 1 μM GoSlo-SR-5-69 (blue bars, Panel F) or 1 μM GoSlo-SR-5-95 (blue bars, Panel I). (For interpretation of the references to colour in this figure legend, the reader is referred to the web version of this article.)

(0.99 mmol) were added. The resulting suspension was capped and irradiated in the microwave oven for 5–20 min at 100–120 °C. The reaction mixture was then cooled to room temperature, filtered and extracted with ethyl acetate (3 × 50 mL). The combined organic layers were dried over anhydrous Na_2SO_4 and concentrated under reduced pressure. The crude residue was purified by silica gel column chromatography (eluted with methanol/ethyl acetate, 1:49 (v/v)) to furnish the anilinoanthraquinone derivatives as blue solids.

5.1.1.1. Sodium 1-amino-4-(cyclopropylamino)-9,10-dioxo-9,10-dihydroanthracene-2-sulfonate, ***3****.* Yield: 39%; ^{1}H NMR (400 MHz, DMSO-d_6, 27 °C): δ 10.51 (d, J = 2.4 Hz, 1H), 10.09 (brs, 1H), 8.27–8.24 (m, 1H), 8.22–8.20 (m, 1H), 8.17 (s, 1H), 7.82–7.80 (m, 2H), 2.80–2.67 (m, 1H), 0.94–0.90 (m, 2H), 0.65–0.62 (m, 2H); ^{13}C NMR (100 MHz, DMSO-d_6, 27 °C): δ 181.67, 181.44, 145.84, 143.43, 143.21, 133.96, 133.73, 132.62, 132.55, 125.89, 125.71, 122.10, 109.19, 109.05, 24.10, 7.63; HRMS (ES): m/z for $C_{17}H_{13}N_2O_5Na_2S$ [M + Na^+], calcd. 403.0341, found 403.0359.

5.1.1.2. Sodium 1-amino-4-(cyclobutylamino)-9,10-dioxo-9,10-dihydroanthracene-2-sulfonate, ***4****.* Yield: 40%; ^{1}H NMR (400 MHz, DMSO-d_6, 27 °C): δ 10.74 (d, J = 6.0 Hz, 1H), 10.10 (brs, 1H), 8.27–8.23 (m, 2H), 7.83–7.80 (m, 2H), 7.64 (s, 1H), 7.41 (brs, 1H), 4.22 (m, 1H), 2.49–2.46 (m, 2H), 2.06–1.96 (m, 2H), 1.90–1.83 (m, 2H); ^{13}C NMR (100 MHz, DMSO-d_6, 27 °C): δ 181.67, 181.09, 143.71, 143.07, 143.04, 133.88, 133.78, 132.62, 132.58, 125.89, 125.69, 121.45, 109.11, 108.84, 47.08, 30.86, 15.03; HRMS (ES): m/z for $C_{18}H_{15}N_2O_5S$ [M − Na^+], calcd. 371.0702, found 371.0692.

5.1.1.3. Sodium 1-amino-9,10-dioxo-4-((5,6,7,8-tetrahydronaphthalen-1-yl)amino)-9,10-dihydroanthracene-2-sulfonate, ***10****.* Yield: 50%; ^{1}H NMR (400 MHz, DMSO-d_6, 27 °C): δ 12.03 (s, 1H), 10.15 (brs, 1H), 8.31–8.28 (m, 2H), 7.88–7.83 (m, 2H), 7.83 (s, 1H), 7.50 (brs, 1H), 7.19 (*t*, J = 7.6 Hz, 1H), 7.09 (d, J = 7.6 Hz, 1H), 7.0 (d, J = 7.2 Hz, 1H), 2.80 (*t*, J = 5.6 Hz, 2H), 2.68 (*t*, J = 5.6 Hz, 2H), 1.81–1.74 (m, 4H); ^{13}C NMR (100 MHz, DMSO-d_6, 27 °C): δ 182.24, 181.71, 143.97, 142.37, 141.96, 138.81, 137.15, 134.03, 133.51, 133.11, 132.79, 130.94, 126.16, 126.01, 125.93, 122.81, 121.40, 110.78, 109.03, 29.16, 24.66, 22.35, 22.12;

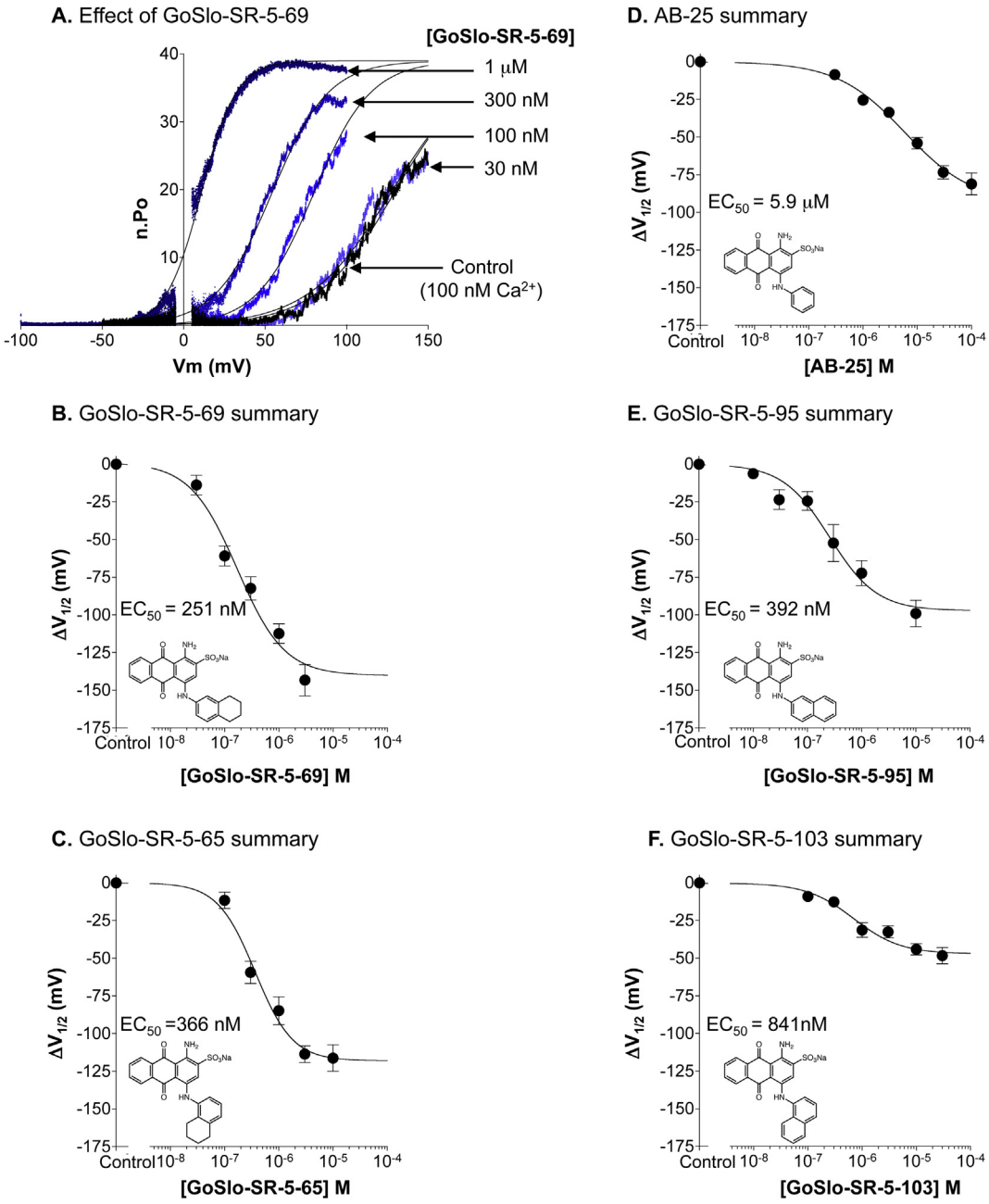

Fig. 5. Comparing potency of the GoSlo-SR molecules with AB-25. (A) Typical BK currents obtained from voltage ramps in response to increasing concentrations of GoSlo-SR-5-69 (blue traces). The solid lines show the Boltzmann fits to the data. (B) A summary plot of the $\Delta V_{1/2}$ (±SEM) obtained from patches bathed in 100 nM Ca^{2+} (Control) before and in the continued presence of increasing concentrations of GoSlo-SR-5-69. The solid lines in (B–F) show the fit to the data obtained with the Langmuir equation. The structure of each compound and its EC_{50} are shown in the inset. For all EC_{50} determinations, different concentrations of each compound were applied to between 5 and 30 patches, with the exception of 300 nM GoSlo-SR-5-103 and AB-25, which were applied to 4 and 2 patches, respectively. As (B) suggests, GoSlo-SR-5-69 was the most potent and efficacious compound of this series and was approximately 24-fold more potent than AB-25 (D). (C) and (E) show that GoSlo-SR-5-65 and GoSlo-SR-5-95 possessed similar potencies and efficacies. As (F) suggests, GoSlo-SR-103 was approximately seven-fold more potent than AB-25, but was less efficacious. (For interpretation of the references to colour in this figure legend, the reader is referred to the web version of this article.)

HRMS (ES): *m*/*z* for $C_{24}H_{19}N_2O_5Na_2S$ [M + Na^+], calcd. 493.0810, found 493.0797.

5.1.1.4. Sodium 1-amino-9,10-dioxo-4-((5,6,7,8-tetrahydronaphthalen-2-yl)amino)-9,10-dihydroanthracene-2-sulfonate, ***12****.* Yield: 76%; ^{1}H NMR (400 MHz, DMSO-d_6, 27 °C): δ 12.07 (s, 1H), 10.15 (brs, 1H), 8.30–8.27 (m, 2H), 7.97 (s, 1H), 7.88–7.82 (m, 2H), 7.49 (brs, 1H), 7.13 (d, J = 8.0 Hz, 1H), 7.02–6.99 (m, 2H), 2.75 (brs, 4H), 1.77 (*t*, J = 2.8 Hz, 4H); ^{13}C NMR (100 MHz, DMSO-d_6, 27 °C): δ 182.04, 181.72, 144.04, 142.43, 141.67, 138.15, 136.11, 134.02, 133.54, 133.07, 132.77, 130.05, 125.99, 125.89, 123.91, 122.80, 121.10, 110.68, 109.01, 28.76, 28.27, 22.66, 22.48; HRMS (ES): *m*/*z* for $C_{24}H_{19}N_2O_5Na_2S$ [M + Na^+], calcd. 493.0810, found 493.0821.

5.1.1.5. Sodium 1-amino-4-((2,3-dihydro-1H-inden-5-yl)amino)-9,10-dioxo-9,10-dihydroanthracene-2-sulfonate, ***14****.* Yield: 66%; ^{1}H NMR (400 MHz, DMSO-d_6, 27 °C): δ 12.10 (s, 1H), 10.15 (brs, 1H), 8.30–8.26 (m, 2H), 7.96 (s, 1H), 7.88–7.81 (m, 2H), 7.50 (brs, 1H), 7.29 (d, J = 8.0 Hz, 1H), 7.15 (s, 1H), 7.04 (dd, J = 2.0, 8.0 Hz, 1H), 2.92–2.88 (m, 4H), 2.11–2.03 (m, 2H); ^{13}C NMR (100 MHz, DMSO-d_6, 27 °C):

δ 181.98, 181.65, 145.48, 144.14, 142.77, 141.90, 140.59, 137.06, 134.09, 133.61, 132.97, 132.67, 125.98, 125.88, 125.12, 122.70, 121.94, 119.90, 110.62, 108.96, 32.44, 31.84, 25.18; HRMS (ES): *m/z* for $C_{23}H_{17}N_2O_5Na_2S$ [M + Na^+], calcd. 479.0654, found 479.0677.

5.1.1.6. Sodium 1-amino-9,10-dioxo-4-((5-oxo-5,6,7,8-tetrahydronaphthalen-2-yl)amino)-9,10-dihydroanthracene-2-sulfonate, ***15***. Yield: 36%; ^{1}H NMR (400 MHz, DMSO-d_6, 27 °C): δ 11.70 (s, 1H), 10.01 (brs, 1H), 8.28–8.22 (m, 2H), 8.16 (s, 1H), 7.90–7.83 (m, 3H), 7.51 (brs, 1H), 7.19–7.16 (m, 2H), 2.93 (*t*, *J* = 6.0 Hz, 2H), 2.59–2.55 (m, 2H), 2.08–2.02 (m, 2H); ^{13}C NMR (100 MHz, DMSO-d_6, 27 °C): δ 196.04, 183.54, 182.27, 146.72, 144.85, 144.75, 141.67, 137.12, 133.99, 133.65, 133.23, 133.02, 128.36, 127.02, 126.06, 124.14, 119.07, 118.29, 114.45, 109.80, 38.37, 29.14, 22.77; HRMS (ES): *m/z* for $C_{24}H_{17}N_2O_6Na_2S$ [M + Na^+], calcd. 507.0603, found 507.0623.

5.1.1.7. Sodium 1-amino-4-((2,3-dihydrobenzo[b] [1,4]dioxin-6-yl) amino)-9,10-dioxo-9,10-dihydroanthracene-2-sulfonate, ***16***. Yield: 60%; ^{1}H NMR (400 MHz, DMSO-d_6, 27 °C): δ 11.99 (s, 1H), 10.15 (brs, 1H), 8.30–8.27 (m, 2H), 7.90 (s, 1H), 7.86–7.84 (m, 2H), 7.49 (brs, 1H), 6.94 (d, *J* = 8.4 Hz, 1H), 6.82 (d, *J* = 2.4 Hz, 1H), 6.77 (dd, *J* = 2.4, 8.8 Hz, 1H), 4.29 (s, 4H); ^{13}C NMR (100 MHz, DMSO-d_6, 27 °C): δ 181.93, 181.64, 144.10, 143.89, 142.86, 142.06, 141.06, 134.09, 133.61, 132.98, 132.68, 132.26, 125.99, 125.87, 122.56, 117.80, 117.37, 112.89, 110.48, 108.92, 64.16, 63.96; HRMS (ES): *m/z* for $C_{22}H_{15}N_2O_7S$ [M − H^+], calcd. 451.0600, found 451.0619.

5.1.1.8. Sodium 1-amino-9,10-dioxo-4-((3-oxo-1,3-dihydroisobenzofuran-5-yl)amino)-9,10-dihydroanthracene-2-sulfonate, ***17***. Yield: 38%; ^{1}H NMR (400 MHz, DMSO-d_6, 27 °C): δ 11.89 (s, 1H), 10.04 (brs, 1H), 8.29–8.25 (m, 2H), 7.98 (s, 1H), 7.88–7.85 (m, 2H), 7.74–7.68 (m, 3H), 7.48 (brs, 1H), 5.44 (s, 2H); ^{13}C NMR (100 MHz, DMSO-d_6, 27 °C): δ 183.04, 182.09, 170.31, 144.40, 142.70, 142.09, 140.61, 139.50, 134.00, 133.46, 133.31, 132.96, 129.16, 126.41, 126.05, 125.99, 124.26, 122.67, 117.50, 112.71, 109.51, 69.92; HRMS (ES): *m/z* for $C_{22}H_{13}N_2O_7S$ [M − Na^+], calcd. 449.0443, found 449.0430.

5.1.1.9. Sodium 1-amino-9,10-dioxo-4-(quinolin-6-ylamino)-9,10-dihydroanthracene-2-sulfonate, ***18***. Yield: 41%; ^{1}H NMR (400 MHz, DMSO-d_6, 27 °C): δ 11.96 (s, 1H), 10.08 (brs, 1H), 8.97 (s, 1H), 8.31–8.26 (m, 3H), 8.14 (s, 1H), 8.07 (d, *J* = 9.2 Hz, 1H), 7.90–7.83 (m, 2H), 7.80 (d, *J* = 2.4 Hz, 1H), 7.73 (dd, *J* = 2.4, 9.2 Hz, 1H), 7.54 (*q*, *J* = 4.0 Hz, 1H); ^{13}C NMR (100 MHz, DMSO-d_6, 27 °C): δ 182.97, 182.01, 149.27, 144.55, 142.34, 139.63, 137.69, 135.27, 134.06, 133.41, 133.38, 132.89, 130.32, 126.37, 126.05, 125.99, 122.99, 118.12, 112.58, 109.44; HRMS (ES): *m/z* for $C_{23}H_{15}N_3O_5NaS$ [M + H^+], calcd. 468.0630, found 468.0630.

5.1.1.10. Sodium 1-amino-9,10-dioxo-4-(quinolin-3-ylamino)-9,10-dihydroanthracene-2-sulfonate, ***19***. Yield: 42%; ^{1}H NMR (400 MHz, DMSO-d_6, 27 °C): δ 12.01 (s, 1H), 10.06 (brs, 1H), 8.91 (s, 1H), 8.31–8.28 (m, 2H), 8.18 (d, *J* = 2.4 Hz, 1H), 8.04 (s, 1H), 8.03 (d, *J* = 7.2 Hz, 1H), 7.93 (d, *J* = 8.4 Hz, 1H), 7.90–7.87 (m, 2H), 7.73–7.61 (m, 2H), 7.50 (brs, 1H); ^{13}C NMR (100 MHz, DMSO-d_6, 27 °C): δ 183.17, 182.10, 147.45, 144.62, 142.42, 139.36, 134.10, 133.49, 133.36, 132.95, 128.47, 128.21, 127.45, 126.09, 126.01, 125.96, 122.49, 113.01, 109.57; HRMS (ES): *m/z* for $C_{23}H_{14}N_3O_5S$ [M − Na^+], calcd. 444.0654, found 444.0653.

5.1.2. General procedure B: preparation of ***7*** *and* ***8***

To a solution of bromaminic acid sodium salt (0.2 g, 0.495 mmol) in water (5 mL) was added copper sulphate (0.1 mmol) and sodium carbonate (0.4 mmol), followed by cycloheptylamine or cyclooctylamine (0.99 mmol). The reaction mixture was stirred for 6–8 h at 105 °C. The reaction mixture was then cooled to room temperature, filtered and extracted with ethyl acetate (3 × 50 mL). The combined organic layers were dried over anhydrous sodium sulphate and concentrated under reduced pressure to obtain the crude residue. The residue was purified by silica gel column chromatography (eluted with methanol/ethyl acetate, 1:49 (v/v)) to furnish the compounds **7** and **8** as blue solids.

5.1.2.1. Sodium 1-amino-4-(cycloheptylamino)-9,10-dioxo-9,10-dihydroanthracene-2-sulfonate, ***7***. Yield: 49%; ^{1}H NMR (400 MHz, DMSO-d_6, 27 °C): δ 10.95 (d, *J* = 7.6 Hz, 1H), 10.18 (brs, 1H), 8.27–8.24 (m, 2H), 7.81–7.79 (m, 2H), 7.75 (s, 1H), 7.40 (brs, 1H), 3.91–3.86 (m, 1H), 2.02–1.96 (m, 2H), 1.70–1.59 (m, 10H); ^{13}C NMR (100 MHz, DMSO-d_6, 27 °C): δ 181.45, 180.58, 144.25, 143.54, 142.96, 133.97, 133.91, 132.45, 132.33, 125.83, 125.69, 121.40, 109.08, 108.67, 52.08, 34.67, 27.57, 23.51; HRMS (ES): *m/z* for $C_{21}H_{21}N_2O_5Na_2S$ [M + Na^+], calcd. 459.0967, found 459.0970.

5.1.2.2. Sodium 1-amino-4-(cyclooctylamino)-9,10-dioxo-9,10-dihydroanthracene-2-sulfonate, ***8***. Yield: 57%; ^{1}H NMR (400 MHz, DMSO-d_6, 27 °C): δ 10.95 (d, *J* = 7.6 Hz, 1H), 10.18 (brs, 1H), 8.27–8.24 (m, 2H), 7.82–7.79 (m, 2H), 7.76 (s, 1H), 7.40 (brs, 1H), 3.92–3.86 (m, 1H), 1.96–1.90 (m, 2H), 1.77–1.59 (m, 12H); ^{13}C NMR (100 MHz, DMSO-d_6, 27 °C): δ 181.45, 180.54, 144.21, 143.48, 142.94, 133.97, 133.90, 132.46, 132.33, 125.83, 125.69, 121.50, 109.11, 108.69, 51.28, 32.21, 26.62, 25.14, 23.06; HRMS (ES): *m/z* for $C_{22}H_{23}N_2O_5S$ [M − H^+], calcd. 427.1328, found 427.1327.

5.1.3. General procedure C: preparation of ***20***–***23***

To a suspension of 1-amino anthraquinone derivative (0.15 mmol) in 1 M HCl (10 mL) was added 1.5 mL aqueous solution of sodium nitrite (0.60 mmol) at 0 °C. The reaction mixture was stirred for 5 min at same temperature and then allowed to stir at room temperature for 1 h. Ten millilitres of ethanol followed by zinc dust (1.5 mmol) were added into the reaction mixture and further stirred at room temperature for 5 min. Reaction mixture was then quenched with 0.5 M sodium bicarbonate solution and extracted with ethyl acetate (2 × 50 mL). Organic layers were dried over anhydrous sodium sulphate and concentrated in vacuo. The crude residue was purified by C_{18}-reversed phase silica gel column chromatography (eluted with water and methanol mixtures). Elution was performed with increased polarity of purified water:-methanol mixtures from 90:10 (% v/v) to 50:50 (% v/v) to furnish the pure deaminated derivative in excellent yield as purple solid.

5.1.3.1. 9,10-Dioxo-4-((5,6,7,8-tetrahydronaphthalen-2-yl)amino)-9,10-dihydroanthracene-2-sulfonic acid, ***20***. Yield: 96%; ^{1}H NMR (400 MHz, DMSO-d_6, 27 °C): δ 11.22 (s, 1H), 8.26 (d, *J* = 7.6 Hz, 1H), 8.20 (d, *J* = 7.2 Hz, 1H), 7.96–7.87 (m, 2H), 7.79 (s, 1H), 7.64 (s, 1H), 7.17 (d, *J* = 8.0 Hz, 1H), 7.08–7.04 (m, 2H), 2.76 (s, 4H), 1.78 (s, 4H); ^{13}C NMR (100 MHz, DMSO-d_6, 27 °C): δ 184.18, 182.43, 154.08, 149.50, 138.24, 135.78, 134.62, 134.30, 134.28, 134.07, 133.78, 132.49, 130.14, 126.60, 126.46, 124.85, 121.92, 115.83, 114.62, 112.65, 28.78, 28.33, 22.64, 22.46; HRMS (ES): *m/z* for $C_{24}H_{18}NO_5S$ [M − H^+], calcd. 432.0906, found 432.0901.

5.1.3.2. 9,10-Dioxo-4-((3-(trifluoromethyl)phenyl)amino)-9,10-dihydroanthracene-2-sulfonic acid, ***22***. Yield: 98%; ^{1}H NMR (400 MHz, DMSO-d_6, 27 °C): δ 11.24 (s, 1H), 8.26 (dd, *J* = 1.2, 7.8 Hz, 1H), 8.21 (dd, *J* = 1.2, 7.4 Hz, 1H), 7.98–7.89 (m, 2H), 7.89 (d, *J* = 1.2 Hz, 1H), 7.76 (d, *J* = 1.2 Hz, 1H), 7.74–7.68 (m, 3H), 7.58 (d, *J* = 6.4 Hz, 1H); ^{13}C NMR (100 MHz, DMSO-d_6, 27 °C): δ 184.49, 182.30, 154.28, 147.61, 140.13, 134.71, 134.36, 134.16, 134.02, 132.49, 130.83, 127.09, 126.67, 126.53, 119.92, 115.90, 115.67, 114.24; HRMS

(ES): *m/z* for $C_{21}H_{11}NO_5F_3S$ [M − H^+], calcd. 446.0310, found 446.0305.

5.1.3.3. 4-((4-Methyl-3-(trifluoromethyl)phenyl)amino)-9,10-dioxo-9,10-dihydroanthracene-2-sulfonic acid, ***23****.* Yield: 96%; ^{1}H NMR (400 MHz, DMSO-d_6, 27 °C): δ 11.19 (s, 1H), 8.26 (d, *J* = 6.8 Hz, 1H), 8.21 (d, *J* = 7.2 Hz, 1H), 7.97–7.89 (m, 2H), 7.85 (d, *J* = 1.2 Hz, 1H), 7.65 (d, *J* = 1.2 Hz, 2H) 7.59–7.54 (m, 2H), 2.46 (s, 3H); ^{13}C NMR (100 MHz, DMSO-d_6, 27 °C): δ 184.38, 182.35, 154.25, 148.30, 137.24, 134.70, 134.27, 134.18, 133.96, 133.62, 132.48, 127.67, 126.64, 126.51, 121.34, 121.28, 115.68, 115.28, 113.73, 18.27; HRMS (ES): *m/z* for $C_{22}H_{13}NO_5F_3S$ [M − H^+], calcd. 460.0467, found 460.0481.

5.2. Computational details for calculating D ring size

To estimate the size of ring D shown in Fig. 2F, calculations were performed within the density functional theory using the B3LYP exchange-correlation functional as implemented in the Gaussian09 program package. Geometry optimizations were performed without any symmetry constraints using the 6-311++g(d,p) basis set. Optimized geometries were characterized as minima by computing the harmonic vibrational frequencies. Coordinates of all optimized compounds are available upon request.

5.3. Rabbit bladder smooth muscle cell preparation

All experiments were approved by the Dundalk Institute of Technology (DkIT) Animal Care and Use Committee and were in accordance with EU legislation. The urinary bladder was removed from both male and female New Zealand White rabbits after they had been killed by intravenous injection of pentobarbitone. The bladder was immediately placed in Krebs' solution, opened up longitudinally and the urothelium removed by sharp dissection. Strips of tissue, 0.5 cm in length, were cut into 1 mm^3 pieces and stored in Hanks Ca^{2+} free solution for 30 min at 4 °C prior to cell dispersal. Smooth muscle cells were isolated from the tissue pieces by ~5 min incubation in a dispersal medium containing (per 5 ml of Ca^{2+} free Hanks solution): 1 mg protease (Sigma type XXIV), 10 mg trypsin inhibitor (Sigma), 10 mg BSA (Sigma) and 15 mg collagenase (Sigma type 1a) while stirring at 35–37 °C.

The tissue suspension was centrifuged at 1000 revolutions min^{-1} for approximately 1 min and the supernatant removed. The tissue pieces were resuspended in Ca^{2+} free Hanks solution and stirred for 6–8 min to release single relaxed smooth muscle cells. The isolated cells were then plated in Petri dishes containing 100 μM Ca^{2+} (which enhanced adherence of the cells to the bottom of the dish) and were stored at 4 °C until use within 8 h.

5.4. Electrophysiology recordings

To screen molecules for biological activity, we utilised voltage ramps to record BK channel openings in inside/out patches of membrane excised from smooth muscle cells isolated from rabbit bladders. Electrodes were pulled from Corning borosilicate glass (1.5 mm O.D. × 0.86 mm I.D.) using a Sutter P-97 pipette puller and were fire polished using a Narashige MF 83 microforge. Standard single channel patch clamp recording methods were used in the inside-out patch conformation [32]. Voltage clamp commands were delivered via either Axopatch 1D or Axopatch 200B patch clamp amplifiers (Axon Instruments) connected to Digidata 1322A AD/DA converters (Axon Instruments) interfaced to a computer running pClamp software (Axon Instruments). Data was acquired at 10 KHz and filtered at 2 kHz. Patches were usually held at −60 mV or −100 mV (as denoted in the text) and the patch potential was ramped from either −150 mV to + 50 mV, −100 mV to +100 mV or −50 to +150 mV over 2 s before returning to −100 mV. These voltage ramps were usually repeated 15 times and the currents were averaged. The currents were divided by the single channel conductance at each voltage and thus corrected for driving force to obtain the number of channels (*n*) multiplied by the open probability (*n*.Po). Maximum *n*.Po was determined by bathing the patch in 1 μM and repeating the voltage ramps. In some examples shown in the presence of 1 μM Ca^{2+}, voltage ramps were only repeated 5–10 times but it was still possible from this to estimate the maximum number of channels in the patch. The data were then fitted with the Boltzmann equation of the form:

$$n.\mathrm{Po} = 1/\left(1+\exp\left(\left(V_{1/2}-V_{\mathrm{patch}}\right)/K\right)\right)$$

where $V_{1/2}$ was the membrane potential at which there was half maximal activation, *K* the slope factor and V_{patch} the patch potential (mV). The change in activation $V_{1/2}$ ($\Delta V_{1/2}$) due to the drugs was obtained by subtracting the $V_{1/2}$ in control from that measured in the presence of the drug. The $V_{1/2}$ is given as the mean ± SEM. The voltage ramps were sufficiently slow (100 mV s^{-1}) so that the activation curves were not distorted by the time constants of activation or deactivation. This analysis provided a continuous recording of the *n*.Po over the entire voltage range [33]. The experiments were carried out between 35 and 37 °C. BK channels were observed in almost every patch and were judged to be BK channels on the basis of their (i) large conductance, (ii) reversal potential at E_K (0 mV), (iii) their calcium and voltage sensitivity, and (iv) their blockade by the selective BK channel blockers, penitrem A, (100 nM) [27] and iberiotoxin.

5.5. Drug delivery

The patches of cell membrane under study were continuously perfused by means of a gravity-fed close delivery system for application of pharmacological agents. A glass micropipette (~100–200 μm in diameter) was attached at the end of the delivery system and its tip placed ~150 μm from the patch. Using this system the flow could be changed over to a solution containing the drug within 5 s. During experimentation, excised patches were bathed with symmetrical K^+ solutions (solution 4) containing 100 nM Ca^{2+}, with or without the relevant drug concentration. Although the physicochemical properties of the GoSlo-SR molecules have not been thoroughly determined, we saw no evidence of aggregation of the drugs in solution when used at concentrations up to 10 μM.

5.6. Solutions for electrophysiology experiments

The following solutions were used. Concentrations in mM are given in parentheses.

A. *Krebs' solution*: NaCl (120), KCl (5.9), $NaHCO_3$ (25), $NaH_2PO_4 \cdot 2H_2O$ (1.2), Glucose (5.5), $MgCl_2$ (1.2), $CaCl_2$ (2.5). pH was adjusted to 7.4 by bubbling the solution with 95% O_2–5% CO_2 continuously.
B. *Ca^{2+} free Hanks solution for cell dispersal*: NaCl (125), KCl (5.4), Glucose (10), Sucrose (2.9), $NaHCO_3$ (4.2), KH_2PO_4 (0.4), NaH_2PO_4 (0.3), Hepes (10). pH was adjusted to 7.4 using NaOH. Solutions 1 and 2 were made up in double distilled water.
C. *100 μM Ca^{2+} H. solution:* $CaCl_2 \cdot 2H_2O$ (0.1 M) in 100 ml of Ca^{2+} free Hanks solution.
D. *Single channel recording solutions:* all recordings were carried out with symmetrical KCl solutions of the following composition (mM): KCl (140), Glucose (10), HEPES (10), EGTA (1) [for

calcium free and 100 nM Ca^{2+}], H-EDTA (1) [for 1 μM Ca^{2+}], pH adjusted to 7.2 using KOH, made up in de-ionised, filtered water obtained from a Milli-Q water purification system. Solutions containing 100 nM Ca^{2+} were used as the pipette solution and the Chelator program [34], was used to calculate the concentration of calcium required to give the desired free $[Ca^{2+}]_i$. Available for download at http://www.ru.nl/organphy/chelator/Chelmain.html

5.7. Statistics

Experiments on freshly dispersed rabbit bladder smooth muscle cells were usually carried out on a minimum of three animals. In all experiments '*n*' refers to the number of patches studied. Summary data are presented as the mean ± SEM and statistical comparisons were made on raw data using students paired or unpaired *t*-test as appropriate, taking $p < 0.05$ level as significant. Concentration–effect data were fitted with a Hill–Langmuir equation of the form:

$$Y = \text{Bottom} + (\text{Top} - \text{Bottom})\left(1 + 10\hat{}((\text{[Drug]} - \text{pEC}_{50})*H)\right)$$

where $\Delta V_{1/2}$ was recorded in the presence of the drug under study, pEC_{50}, was the −log of the half maximal effective concentration, [Drug] is the agonist concentration variable and *H* was the Hill coefficient.

Conflict of interest statement

K. D. Thornbury, N. G. McHale, G. P. Sergeant, S. Roy and M. A. Hollywood have submitted a Patent application (IPN WO 2012/035122 A11) on this family of molecules.

Author contributions

SR performed synthesis and characterization of the compounds. RL, AMA and AK performed the electrophysiology experiments. CD performed atomic calculations. RL, AK, AMA & MAH analysed the data. All authors designed experiments, contributed to and approved the final manuscript.

Acknowledgements

This work was funded by Enterprise Ireland's Applied Research Enhancement Scheme. A. M. Akande was funded by a Council of Directors Strand 1 Award and DkIT Research Office. A.K was supported by Science Foundation Ireland under their Research Frontiers Programme. C. Domene would like to acknowledge the use of the EPSRC UK National Service for Computational Chemistry Software (NSCCS) at Imperial College London in carrying out the computational work. We would also like to thank Shanghai YoungLong Chem-Tech Co., Ltd. for supplying Acid Blue 62 as a gift.

The funding agencies did not participate in study design; in the collection, analysis and interpretation of data; in the writing of the report; or in the decision to submit the article for publication. We would like to thank the Royal College of Surgeons in Ireland for use of their NMR facility and Billie McIlveen for excellent technical assistance.

Appendix A. Supplementary data

Supplementary data related to this article can be found at http://dx.doi.org/10.1016/j.ejmech.2014.01.035.

References

[1] L. Salkoff, A. Butler, G. Ferreira, C. Santi, A. Wei, Nat. Rev. Neurosci. 7 (2006) 921–931.
[2] H. Hu, L.R. Shao, S. Chavoshy, N. Gu, M. Trieb, R. Behrens, P. Laake, O. Pongs, H.G. Knaus, O.P. Ottersen, J.F. Storm, J. Neurosci. 21 (2001) 9585–9597.
[3] G. Raffaelli, C. Saviane, M.H. Mohajerani, P. Pedarzani, E. Cherubini, J. Physiol. 557 (2004) 147–157.
[4] Z.W. Wang, Mol. Neurobiol. 38 (2008) 153–166.
[5] Y. Imaizumi, S. Henmi, Y. Uyama, K. Atsuki, Y. Torii, Y. Ohizumi, M. Watanabe, Am. J. Physiol. 271 (1996) C772–C782.
[6] T.B. Bolton, Y. Imaizumi, Cell. Calcium 20 (1996) 141–152.
[7] U. Klokner, G. Isenberg, Pflugers Arch. 405 (1985) 329–339.
[8] A.G. Davies, J.T. Pierce-Shimomura, H. Kim, M.K. VanHoven, T.R. Thiele, A. Bonci, C.I. Bargmann, S.L. McIntire, Cell 115 (2003) 655–666.
[9] M. Guest, K. Bull, R.J. Walker, K. Amliwala, V. O'Connor, A. Harder, L. Holden-Dye, N.A. Hopper, Int. J. Parasitol. 37 (2007) 1577–1588.
[10] L. Holden-Dye, V. O'Connor, N.A. Hopper, R.J. Walker, A. Harder, K. Bull, M. Guest, Invert. Neurosci. 7 (2007) 199–208.
[11] T.J. Heppner, A.D. Bonev, M.T. Nelson, Am. J. Physiol. 273 (1997) C110–C117.
[12] B. Kyle, E. Bradley, S. Ohya, G.P. Sergeant, N.G. McHale, K.D. Thornbury, M.A. Hollywood, Am. J. Physiol. Cell. Physiol. 301 (2011) C1186–C1200.
[13] H. Hashitani, H. Fukuta, H. Takano, M.F. Klemm, H. Suzuki, J. Physiol. 530 (2001) 273–286.
[14] H. Hashitani, A.F. Brading, Br. J. Pharmacol. 140 (2003) 159–169.
[15] K.L. Hristov, M. Chen, W.F. Kellett, E.S. Rovner, G.V. Petkov, Am. J. Physiol. Cell. Physiol. 301 (2011) C903–C912.
[16] K.L. Hristov, S.A.Y. Afeli, S.P. Parajuli, Q. Cheng, E.S. Rovner, G.V. Petkov, PLoS One 8 (2013) e68052.
[17] K.L. Hristov, S.P. Parajuli, R.P. Soder, Q. Cheng, E.S. Rovner, G.V. Petkov, Am. J. Physiol. Cell. Physiol. 302 (2012) C1632–C1641.
[18] A.L. Meredith, K.S. Thorneloe, M.E. Werner, M.T. Nelson, R.W. Aldrich, J. Biol. Chem. 279 (2004) 36746–36752.
[19] T.M. Argentieri, J.A. Butera, Expert Opin. Ther. Pat. 16 (2006) 573–585.
[20] M.L. Garcia, D.M. Shen, G.J. Kaczorowski, Expert Opin. Ther. Pat. 17 (2007) 831–842.
[21] A. Nardi, V. Calderone, S.P. Olesen, Lett. Drug. Des. Dis. 3 (2006) 210–218.
[22] A. Nardi, S.P. Olesen, Exp. Opin. Ther. Pat. 17 (2007) 1215–1226.
[23] A. Nardi, S.P. Olesen, Curr. Med. Chem. 15 (2008) 1126–1146.
[24] S. Roy, A.M. Akande, R.J. Large, T.I. Webb, C. Camarasu, G.P. Sergeant, N.G. McHale, K.D. Thornbury, M.A. Hollywood, Chem Med Chem 7 (2012) 1763–1769.
[25] D. Strøbaek, P. Christophersen, N.R. Holm, P. Moldt, P.K. Ahring, T.E. Johansen, S.P. Olesen, Neuropharmacology 35 (1996) 903–914.
[26] B.H. Bentzen, A. Nardi, K. Calloe, L.S. Madsen, S.P. Olesen, M. Grunnet, Mol. Pharmacol. 72 (2007) 1033–1044.
[27] H. Knaus, O. McManus, S. Lee, W. Schmalhofer, M. Garcia-Calvo, L. Helms, M. Sanchez, K. Giangiacomo, J. Reuben, A. Smith, G. Kaczorowski, M. Garcia, Biochemistry 33 (1994) 5819–5828.
[28] Y. Baqi, C.E. Müller, Org. Lett. 9 (2007) 1271–1274.
[29] Y. Baqi, S. Weyler, J. Iqbal, H. Zimmermann, C.E. Müller, Pur. Signal 5 (2009) 91–106.
[30] Y. Baqi, S.Y. Lee, J. Iqbal, P. Ripphausen, A. Lehr, A.B. Scheiff, H. Zimmermann, J. Bajorath, C.E. Müller, J. Med. Chem. 53 (2010) 2076–2086.
[31] Y. Baqi, C.E. Müller, Tetrahedron Lett. 53 (2012) 6739–6742.
[32] O.P. Hamill, A. Marty, E. Neher, B. Sakmann, F.J. Sigworth, Pflügers Arch. 391 (1981) 85–100.
[33] A. Carl, K.M. Sanders, J. Neurosci. Methods 33 (1990) 157–163.
[34] T.J. Schoenmakers, G.J. Visser, G. Flik, A.P. Theuvenet, Biotechniques 12 (1992) 870-874–876-879.